

A Numerical Analysis on Heat Inflow into a Rectangular Cavity

Kyung-Jin Lee* and Won-Gee Chun**

사각형상 공동으로의 열유입에 관한 수치해석 연구

이 경 진* · 천 원 기**

ABSTRACT

A numerical experiment about thermal discharge into a rectangular shaped enclosed body of fluid that has one inlet and one outlet jet has been carried out. Three two-dimensional partial differential equations (the heat transport equation, vorticity transport equation and stream function equation) that are coupled by the nature of the problem were solved by using the Alternating Direction Implicit method and Successive Over-Relaxation. A computer program was developed on the basis of these algorithms to give the temperature and velocity distribution at each time step. The results are then reviewed in terms of the physical parameters involved. The numerical stability of the scheme is also discussed.

Depending on the actual boundary conditions, the numerical results obtained could provide some information to predict the flow pattern and thermal penetration within the lower convective zone of a salt-stratified solar pond as well as inside the heat storage units of other heat collection systems.

Key words : Numerical experiment, Vorticity transport equation,
Alternating direction implicit method

1. Introduction

The problem of thermal discharge into an enclosed body of fluid has drawn a great deal of attention in

recent years, since it describes the physical phenomenon that arises in the lower convective zone of a salt-stratified solar pond associated with decanting schemes and in other heat storage units of solar thermal systems. Quite a number of papers were published, which employed the numerical experiments to probe and understand this natural phenomenon. Most of the studies carried out the analyses on a

* 제주대학교 대학원
Graduate School, Cheju Nat'l Univ.
** 제주대학교 에너지공학과
Dept. of Nuclear and Energy Eng., Cheju Nat'l Univ.

rectangular shape of fluid body with at least one inlet and one outlet jet for various boundary conditions. Cabelli⁽¹⁾ set up a two-dimensional model to simulate the motion which takes place in storage tanks. He tried to test the validity of the one-dimensional model. A one-dimensional model has been often used to simulate solar water heating systems. Newell⁽²⁾ developed an explicit finite difference numerical model capable of solving transient, double diffusive fluid problems within a cavity. He examined the transient effects of decanting schemes within the storage zone of a solar pond. However, warns the propagation of catastrophic instabilities which might rise from such restricted boundary conditions.

The effect of inlet and outlet jet placement is extensively studied by many, since the characteristics of the flow field largely depend upon the arrangement of the jets.

There are certain simplifying assumptions that have to be made regarding the motion and dynamics of flow, otherwise the mathematical relationships which describe the effect of forced and natural convection are too difficult to solve. The two-dimensional flow assumption and Boussinesq approximation are those frequently introduced to meet this purpose. Assuming the motion of fluid being two-dimensional might raise some skepticism. Jaluria and Cha⁽⁴⁾ have explained the validity of this assumption in detail : "The two-dimensional flow assumption is made since it is desirable to spread out the flow over the entire storage region and keep the flow velocities low, particularly in a solar pond where large velocities could lead to the destabilization of the gradient zone. In practice, the flow will tend to be three-dimensional near the inlet and outlet. But if several inlet and outlet ports are positioned linearly, the flow will be largely two-dimensional in most of the flow region. " The Boussinesq approximation is used by many to

account for the buoyant influence in the momentum equation, which assumes the density to be constant everywhere except as it affects the buoyant forces. Even though the fluid motion is the result of density variations, these variations are quite small, and a satisfactory solution to the problem may be obtained by assuming incompressible flow⁽⁵⁾. Leonardi and Reizes⁽⁶⁾ showed the accuracy of this assumption in their numerical experiment on the convective flows in closed cavities. They also showed how accurate it is to assume constant properties with Boussinesq approximation.

The primitive forms of the governing equations involved in this problem could be reduced in terms of stream function and vorticity by doing several steps of mathematical manipulation to eliminate the pressure terms in the momentum equations. These alternative forms of the governing equations constitute the stream function-vorticity formulation, which is employed in the following analysis to pursue the numerical experiment. However, some of the analyses have been carried out with the primitive forms of the governing equations rather than the stream function-vorticity formulation. Four equations (two momentum equations, continuity equation and heat transport equation) have to be solved if primitive variables (velocity, pressure) were used while the stream function-vorticity formulation needs only three equations to be solved. These are the vorticity transport equation, heat transport equation and stream function equation. The stream function equation has the form of the so-called Poisson equation. The striking advantage of the stream function-vorticity formulation is the fact that only one momentum equation be treated.

The Alternating Direction Implicit method (ADI method) is one of the most widely used algorithms to solve the transport equations of the stream function-vorticity formulation. This method was introduced by Peaceman and Rachford⁽⁷⁾ in 1955.

The basic feature of this method is the changing of rows and columns for each successive time step so that, numerically speaking, the difference expression of a partial differential equation is implicit in one direction at the first time step and in the other direction at the second time step. The advantage of this approach over the fully implicit methods is that each equation, although implicit, be only tri-diagonal. In other words, the method requires only the solution of a tri-diagonal system which occurs only for usual implicit methods in one dimension. This reduces the overall computation time to a fraction of what would be needed if fully implicit method were used.

While the ADI method provides numerical means to solve the transport equations relatively easily, the iterative technique of Successive Over-Relaxation (SOR) could handle the Poisson equation without excessive roundoff error problems. The SOR method usually saves computation time by accelerating the already convergent iterative process.

II. Analysis

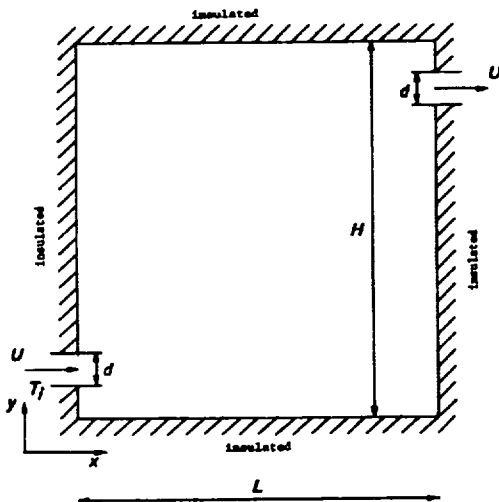


Fig. 1 The geometry of the problem

The physical situation and the coordinate system chosen for the analysis are illustrated in Figure 1. Besides the configuration shown, various cases are considered for the placement of the jets. The fluid is initially motionless and at a uniform temperature of T_0 . The objective of the analysis is to observe the development of the flow field and the temperature distribution within the fluid body due to the sudden onset of the jets. The governing equations involved are given as:

momentum equation

$$\frac{\partial u}{\partial t} + u \frac{\partial u}{\partial x} + v \frac{\partial u}{\partial y} = -\frac{1}{e} \frac{\partial p}{\partial x} + \nu \left(\frac{\partial^2 u}{\partial x^2} + \frac{\partial^2 u}{\partial y^2} \right) \quad (1)$$

$$\frac{\partial v}{\partial t} + u \frac{\partial v}{\partial x} + v \frac{\partial v}{\partial y} = -\frac{1}{e} \frac{\partial p}{\partial y} + \nu \left(\frac{\partial^2 v}{\partial x^2} + \frac{\partial^2 v}{\partial y^2} \right) + g\beta(t - t_0) \quad (2)$$

energy equation

$$\frac{\partial T}{\partial t} + u \frac{\partial T}{\partial x} + v \frac{\partial T}{\partial y} = \alpha \left(\frac{\partial^2 T}{\partial x^2} + \frac{\partial^2 T}{\partial y^2} \right) \quad (3)$$

continuity equation

$$\frac{\partial u}{\partial x} + \frac{\partial v}{\partial y} = 0 \quad (4)$$

These equations are derived on the basis of the following assumptions:

- (a) The flow is two-dimensional and laminar.
- (b) The physical properties of the fluid are constant except as they affect the gravitational term in the y-direction momentum equation (Boussinesq approximation).
- (c) Viscous dissipation and compressibility effects are neglected.

The boundary conditions for the above equations

could be imposed in many ways. However, rather simpler cases are considered as follows:

- (a) The flow is uniform with a velocity U at the inlet and outlet jets.
- (b) The temperature at the inflow is known as T_i .
- (c) There is no slippage at the walls.
- (d) The enclosure is totally insulated.

If the heat storage zone of a salt stratified solar pond is simulated, zero shear would be more suitable than the nonslip condition for the upper surface. The pressure terms in equations (1) and (2) may be eliminated by several steps of mathematical manipulation. First, differentiate equations (1) and (2) with respect to y and x , respectively. Second, subtract (2) from (1) and apply (4). This gives the following equations:

$$\begin{aligned} & \frac{\partial}{\partial t} \left(\frac{\partial u}{\partial y} - \frac{\partial v}{\partial x} \right) + u \frac{\partial}{\partial x} \left(\frac{\partial u}{\partial y} - \frac{\partial v}{\partial x} \right) + \\ & v \frac{\partial}{\partial y} \left(\frac{\partial u}{\partial y} - \frac{\partial v}{\partial x} \right) = \nu \left[\frac{\partial^2}{\partial x^2} \left(\frac{\partial u}{\partial y} - \frac{\partial v}{\partial x} \right) + \right. \\ & \left. \frac{\partial^2}{\partial y^2} \left(\frac{\partial u}{\partial y} - \frac{\partial v}{\partial x} \right) \right] - g\beta \frac{\partial T}{\partial x} \end{aligned}$$

Finally, the introduction of vorticity w called vorticity $\omega = \frac{\partial v}{\partial x} - \frac{\partial u}{\partial y}$ produces the so-called vorticity transport equation:

$$\begin{aligned} & \frac{\partial \omega}{\partial t} + u \frac{\partial \omega}{\partial x} + v \frac{\partial \omega}{\partial y} \\ & = \nu \left(\frac{\partial^2 \omega}{\partial x^2} + \frac{\partial^2 \omega}{\partial y^2} \right) + g\beta \frac{\partial T}{\partial x} \end{aligned} \quad (5)$$

The two-dimensional flow assumption enables the application of the stream function into the problem and produces the following additional equations:

$$u = \frac{\partial \psi}{\partial y}, \quad v = -\frac{\partial \psi}{\partial x} \quad (6)$$

$$\left(\frac{\partial^2 \omega}{\partial x^2} + \frac{\partial^2 \omega}{\partial y^2} \right) = -\omega \quad (7)$$

Equation (7) is obtained by merely incorporating equation (6) with the definition of vorticity, which is an elliptic Poisson equation. The equations are now nondimensionalized in terms of the following dimensionless variables

$$\begin{aligned} X &= \frac{x}{d}, \quad Y = \frac{y}{d}, \\ \bar{u} &= \frac{u}{U}, \quad \bar{v} = \frac{v}{U}, \\ \theta &= \frac{T - T_0}{T_i - T_0}, \quad \tau = \frac{t}{d \left(\frac{d}{U} \right)}, \\ \phi &= \frac{\psi}{dU}, \quad \Omega = \frac{\omega}{U/d} \end{aligned}$$

The nondimensional forms of the governing equations are :

vorticity transport equation

$$\begin{aligned} & \frac{\partial \Omega}{\partial \tau} + \bar{u} \frac{\partial \Omega}{\partial X} + \bar{v} \frac{\partial \Omega}{\partial Y} = \\ & \frac{1}{Re} \left(\frac{\partial^2 \Omega}{\partial X^2} + \frac{\partial^2 \Omega}{\partial Y^2} \right) + \frac{Gr}{(Re)^2} \frac{\partial \theta}{\partial X} \end{aligned} \quad (8a)$$

or

$$\begin{aligned} & \frac{\partial \Omega}{\partial \tau} = \frac{\partial}{\partial X} \left(-\frac{1}{Re} \frac{\partial \Omega}{\partial X} - \bar{u}\Omega \right) + \\ & \frac{\partial}{\partial Y} \left(-\frac{1}{Re} \frac{\partial \Omega}{\partial Y} - \bar{v}\Omega \right) + \frac{Gr}{(Re)^2} \frac{\partial \theta}{\partial X} \end{aligned} \quad (8b)$$

heat transport equation

$$\begin{aligned} & \frac{\partial \theta}{\partial \tau} + \bar{u} \frac{\partial \theta}{\partial X} + \bar{v} \frac{\partial \theta}{\partial Y} = \\ & \frac{1}{Pe} \left(\frac{\partial^2 \theta}{\partial X^2} + \frac{\partial^2 \theta}{\partial Y^2} \right) \end{aligned} \quad (9a)$$

or

$$\begin{aligned} & \frac{\partial \theta}{\partial \tau} = \frac{\partial}{\partial X} \left(\frac{1}{Pe} \frac{\partial \theta}{\partial X} - \bar{u}\theta \right) + \\ & \frac{\partial}{\partial Y} \left(\frac{1}{Pe} \frac{\partial \theta}{\partial Y} - \bar{v}\theta \right) \end{aligned} \quad (9b)$$

stream function equation

$$\frac{\partial^2 \phi}{\partial X^2} + \frac{\partial^2 \phi}{\partial Y^2} = -\Omega \quad (10)$$

The transport equations in their nonconservative forms, 8(a) and 9(a), are likely to result in an appreciable disturbance of the heat-flux balance at the boundaries of the computation region for strongly nonuniform temperatures. For this reason

the divergence forms 8(b) and 9(b), which are conservative, are used. The vorticity and heat transport equations are parabolic, while the stream function equation is elliptic. The equations are coupled with one another as shown. Besides the nonlinear terms in the transport equations, this coupled nature of the problem makes it impossible to obtain the analytical solution.

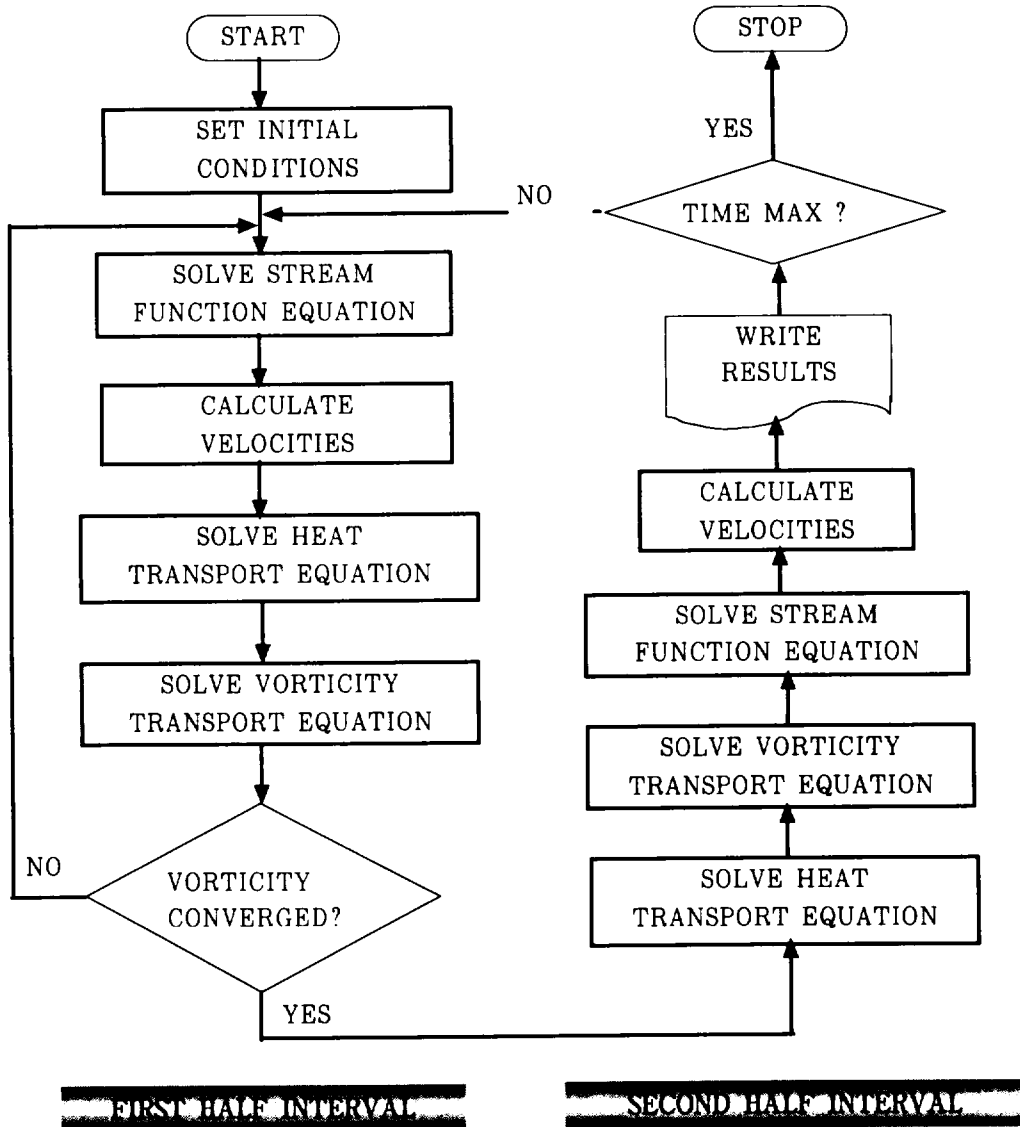


Fig. 2 Flowchart

The equations (8), (9) and (10) are solved by numerical methods with the following nondimensionalized boundary conditions :

$$\begin{aligned} \bar{u}(X, Y, 0) = \bar{v}(X, Y, 0) = \theta(X, Y, 0) = 0 \\ \bar{u}(X, 0, \tau) = \bar{v}(X, 0, \tau) = \theta(X, 0, \tau) = 0 \\ \bar{v}(X, H/d, \tau) = \frac{\partial \theta}{\partial Y}(X, H/d, \tau) = 0 \\ \bar{u}(X, H/d, \tau) = 0 \text{ or } \frac{\partial \bar{u}}{\partial Y}(X, H/d, \tau) = 0 \\ \bar{v}(0, Y, \tau) = \frac{\partial \theta}{\partial X}(0, Y, \tau) = 0 \\ \bar{u}(0, Y, \tau) = 0 \text{ except at the inlet where } \\ \quad \quad \quad \bar{u} = 1 \\ \theta = 1 \text{ at the inlet} \\ \bar{v}(L/d, Y, \tau) = \frac{\partial \theta}{\partial X}(L/d, Y, \tau) = 0 \\ \bar{v}(L/d, Y, \tau) = 0 \text{ except at the outlet where } \\ \quad \quad \quad \bar{u} = 1 \end{aligned}$$

Finite differences are used to approximate the equations and the boundary conditions. These approximations are then applied to a finite number of grid points including the boundaries. The transport equations are solved by the Alternating Direction Implicit method.

III. Finite Difference Scheme

The solution domain is divided into a finite number of uniform rectangular grids. An approximation to the solution will be obtained at grid points whose coordinates are denoted by the integer variables i and j where

$$\begin{aligned} X &= (i-1)\Delta X \quad 1 \leq i \leq M, \\ Y &= (j-1)\Delta Y \quad 1 \leq j \leq N, \\ \Delta X &= L/(M-1)d \\ \text{and} \\ \Delta Y &= H/(N-1)d. \end{aligned}$$

Let k denote the number of time steps and $\Delta \tau$ the size of the time step. Values of variables at grid points are denoted by using i, j (subscripts) and

k (superscript).

The calculation of temperature and vorticity fields at $\tau = (k+1)\Delta \tau$ requires the knowledge of these fields at $\tau = k\Delta \tau$. Suppose that all quantities are known at a time $\tau = k\Delta \tau$ ($k=0$ corresponds to the initial condition). The ADI method is employed to advance the temperature and vorticity fields across a time step $\Delta \tau$ to the new level $(k+1)\Delta \tau$.

IV. Results and Discussion

The two-dimensional numerical scheme employed here has predicted the rapid establishment of the flow field. This could be easily seen by examining the development of the stream function field. Once the flow field is established, it changes very little as time elapses. Figures 3 and 4 show such development. To reach $\tau = 1.0$ (dimensionless time) with an increment of $\tau = 0.0005$, 3.7 hours of CPU time were consumed. With $\tau = 0.0001$, 16 hours of CPU time were needed. Here all the numerical results are generated on a 41 x 41 grid system.

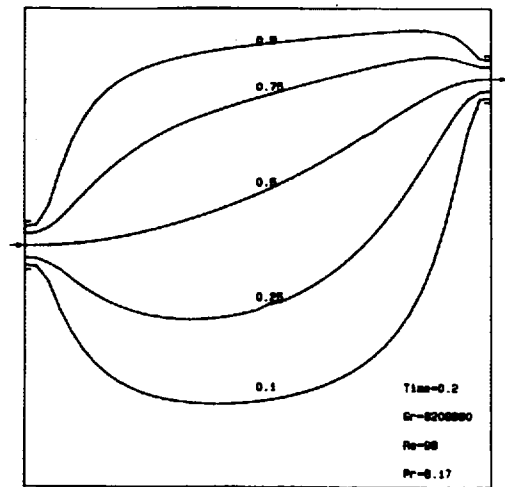


Fig. 3 Streamlines(time=0.2)

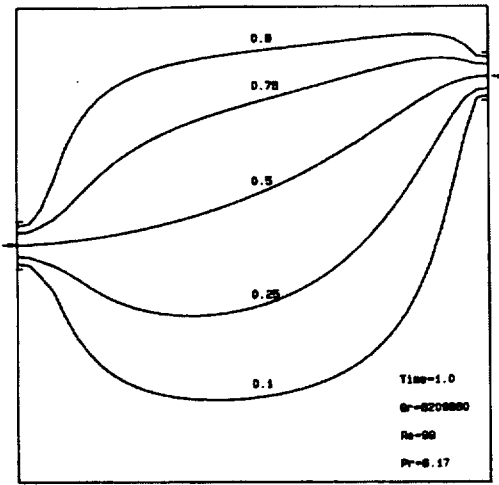


Fig. 4 Streamlines(time =1.0)

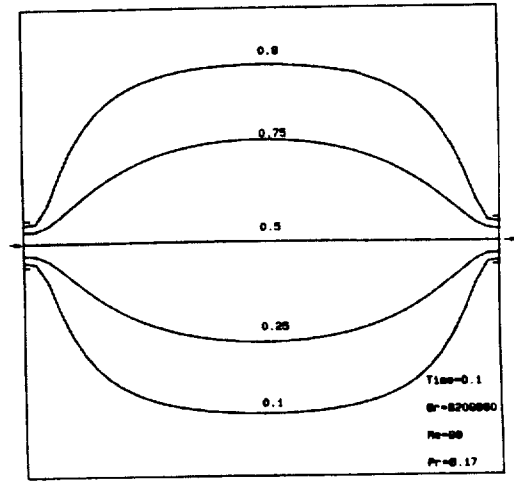


Fig. 6 Streamlines(time =0.1)

The placement of the inlet and outlet jets is very important in that it essentially determines the overall configuration of the flow field. Figures 5, 6 and 7 feature some of the flow field with different jet placements. If the decanting scheme of a solar pond is considered, it would be desirable to have both the inlet and outlet ports on the same side

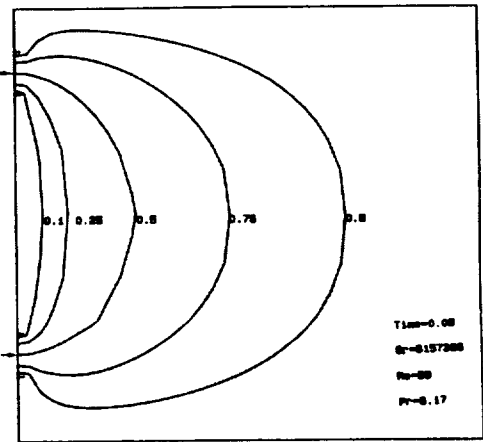


Fig. 7 Streamlines(time =0.05)

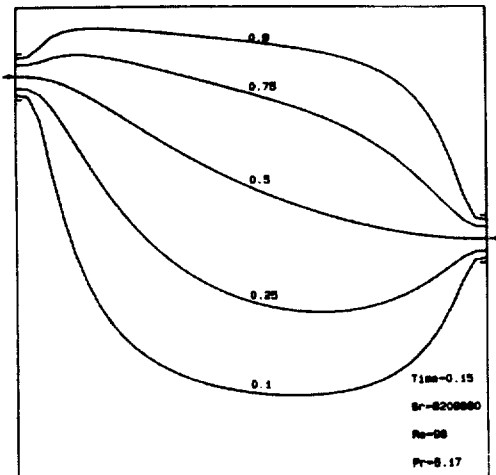


Fig. 5 Streamlines(time =0.15)

rather than placing one of the ports on the opposite end. This could save the cost of piping considerably. However, it is likely to extract less energy from the storage zone unless the horizontal dimension of the pond is within its maximum thermal penetration length.

The implicit scheme of ADI seems to have some restriction on time step (increment) especially when the method of Wilkes and Churchill⁽⁸⁾ is employed.

This is mainly due to the lag of wall vorticity values: Wilkes and Churchill have used the stream function field of the previous time step to calculate the wall vorticity values at the next time step. They assumed that the old boundary vorticities remain valid for the computation of the new interior vorticities. As mentioned earlier, the boundary vorticities are implicitly related to the stream function field. For large time steps, the solution eventually converged to an unreasonable solution or did not converge at all. Here the unreasonable solution indicates the physically impossible solution. Nogotov⁽⁹⁾, who developed the scheme used here, suggests that method is stable if

$$\frac{2}{\Delta\tau} > \max_{i,j} \left(\frac{u_{i-\frac{1}{2},j} - u_{i+\frac{1}{2},j}}{h}, \frac{v_{i,j-\frac{1}{2}} - v_{i,j+\frac{1}{2}}}{h} \right)$$

However, should the lag of wall vorticity values be considered, the time step $\Delta\tau$ must be smaller than this value. Besides the restriction on time step due to the lag of wall vorticity values, the upwind difference scheme used here suffers from instabilities when the Grashof number exceeds a certain limit. This limit for the Grashof number seems to exist around 10^8 . Once the limit is exceeded very far, the disturbances start to set in around the inlet region and propagate throughout the whole solution domain. Velocities show a total chaos, changing their signs and magnitudes in a random manner—this is, of course, due to the stream function field. Reducing the time step only delays the occurrence of such catastrophic instabilities. A parabolic velocity profile, rather than uniform velocity, imposed at the inlet has accelerated the onset of such instabilities about 1.4 times faster. Generally, dynamic instabilities are caused by large time steps while static instabilities result from the finite difference scheme employed. The former can be eliminated by reducing time

steps and the latter can be prevented by imposing some restriction on the Reynolds number as well as Grashof number. Reducing the effect of buoyancy in the vorticity transport equation by increasing the Reynolds number does not necessarily stabilize the numerical solution, since there is also a limitation on the Reynolds number. The present scheme was stable up to $Gr = 10^7$ when $Re = 250$.

Three alternatives were examined to set the values of vorticities at the sharp convex corners (the inlet and outlet ports). All three were tested with uniform inflow and outflow conditions. The first choice was to set zero vorticities there, since the upstream (downstream for the outflow) is uniform flow. The second was to treat these nodes as singular points and to use downstream (upstream for the outflow) values of the stream function in calculating vorticities there. Finally, the average values of both the first and second case were used. In contrast to what was anticipated all three cases produced almost identical results.

In Figures 8 and 9, the numerical results from the present scheme are compared with those in the Figure 2 of Jaluria and Gupta⁽⁹⁾ when $Gr = 2500$ and $Re = 50$ (Physically such a small Grashof

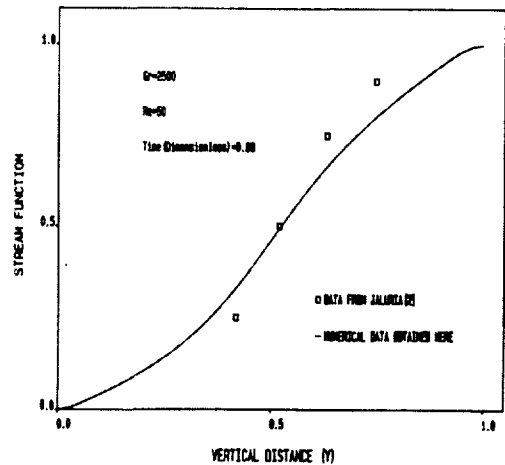


Fig. 8 Stream function vs Y(at X=0.25)

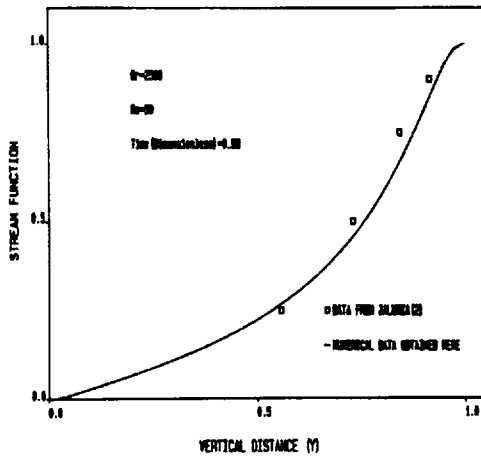


Fig. 9 Stream function vs Y (at X=0.75)

number and a small Reynolds number have no significant meaning: when $H = 2m$, $L = 2m$, $d = 0.1m$ and the properties of the brine are used, ΔT should be less than $0.001^\circ C$). Each plot shows the distribution of the stream function field along vertical direction. As the comparison is made further downstream from the inflow region, they show better agreement.

In addition to the implicit upwind differencing approach discussed above, there were two other schemes tested to solve the transport equations during this experiment. One of them was a fully explicit upwind differencing scheme. This method has produced very close results with the ADI scheme finally adopted here. However the method was abandoned, in spite of its simplicity to program, because of a severe restriction on time step size. It took at least as much as six times more CPU time than the present implicit scheme and was more susceptible to instabilities.

V. Conclusion

The results obtained throughout this numerical

experiment show good agreement with the previous investigations. The ADI method used here to solve the transport equations was considerably faster than any explicit scheme.

The time lag of boundary vorticities has imposed a severe restriction on time step (increment) when the method of Wilkes and Churchill is employed. However, this method is as fast as the one with a large time step because the latter requires a number of iterations over each time step to overcome the lag of boundary vorticities. There are a number of problems merged during this numerical experiment. First of all, it is not certain why the parabolic velocity profile at the inlet has accelerated (compare to the case of slug flow) the instabilities when Grashof number exceeds its stability limit. Second, there are various ways to set the values of vorticities for convex (sharp) corners. It is not clear which one is the best for the case considered here. Finally, the applicability of a variable grid system can be examined, the finer ones around the region where the mass transfer takes place. Grashof number has little influence in stabilizing the numerical solution as long as the Reynolds number is kept high.

References

- 1) Cabell, A., 1977, "Storage Tanks—A Numerical Experiment, Solar Energy," Vol. 19, No. 1-D, pp. 45-54.
- 2) Newell, T. A., "Investigation of Salt Stratified Solar Pond Operational Characteristics," Ph. D. Dissertation, University of Utah.
- 3) Roache, P. J., 1982, Computational Fluid Dynamics, 1st ed., Hermosa Publishers, Albuquerque, pp. 1-277.
- 4) Jaluria, Y. and Cha, C. K., 1983, "Heat Rejection to the Surface Layer of a Solar

- Pond." ASME Paper 83-HT-77.
- 5) Holman. J. P., 1976. Heat Transfer. 5th ed., McGraw-Hill, New York, pp. 26E:-267.
 - 6) Leonardi, E. and Reizes, J. A., 1931. "Convective Flow in Closed Cavities with Variable Fluid Properties," Numerical Methods in Heat Transfer 1st ed., Lewis, R. W., Morgan, K. and Zienkiewics, O. C., eds., John Wiley & Sons Ltd., New York, pp. 387-412.
 - 7) Peaceman, D. W. and Tachford, H. H., Jr., 1955. "The Numerical Solution of Parabolic and Elliptic Differential Equations." J. Soc. Indus. Appl. Math., Vol. 3, No. 1, pp. 28-41
 - 8) Wilkes, J. O. and Churchill, S. W., 1966. "The Finite Difference Computation of Natural Convection in a Rectangular Enclosure." A. I. Ch. E. Journal, Vol. 12, No. 1, January pp. 161-166.
 - 9) Runchal, A. K. and Wolfshtein, M., 1969. "Numerical Integration Procedure for the Steady State Navier-Stokes Equations." J. Mech. Eng. Sci., Vol. 11, No. 5, pp. 445-453.